GAMMA-RAY BURST OBSERVATIONS WITH *FERMI*

F. PIRON
on behalf of the *Fermi* LAT Collaboration
Laboratoire Univers et Particules de Montpellier,
Université Montpellier 2, CNRS/IN2P3, Montpellier, France

After more than four years of science operation, the Large Area Telescope (LAT) onboard the *Fermi* Gamma-Ray Space Telescope has detected emission from more than 35 Gamma-Ray Bursts (GRBs) at energies ranging from 20 MeV up to tens of GeV. We give an overview of these observations, focusing on the 3-year LAT GRB catalog and presenting the common properties in GRB temporal and spectral behavior at high energies. We also highlight the unique characteristics of some individual bursts. The main physical implications of these results are discussed, along with open questions regarding GRB modeling in their prompt and temporally-extended emission phases.

1 Introduction

The *Fermi* Large Area Telescope [11] (LAT) is a pair-conversion detector of high-energy gamma rays of energies ranging from 20 MeV to more than 300 GeV. Since the launch in June 2008, it has been operating in synergy with the Gamma-ray Burst Monitor [22] (GBM), which covers the entire unocculted sky and is designed for gamma-ray transients' detection and spectroscopy between 8 keV and 40 MeV.

This review covers the LAT observational results, focusing on recent populations studies and on GRB common properties at high energies. In section 2, we present what has been seen with the LAT in 3 years of operations, highlighting results from the first LAT GRB catalog. In section 3, we discuss the LAT GRB rate and examine the LAT non-detections of GBM bright GRBs. Whereas about half of the GBM GRBs occur in the LAT field of view (FoV), we investigated why only ~8% are detected with the LAT above 100 MeV. We give our conclusions and some perspective in section 4.

2 The First LAT Gamma-Ray Burst Catalog

The first LAT GRB catalog, which is presented in detail in Ref. [18], is a systematic study of GRBs at high energies (>20 MeV), covering a 3-year period starting from the beginning of the nominal *Fermi* science operations in August 2008. It aims at characterizing GRB temporal and spectral properties at high energies, including tabulated GRB parameters along with details on the analysis methodology and tools and their caveats. In the following, we describe some of the ingredients necessary to this work and present selected results.

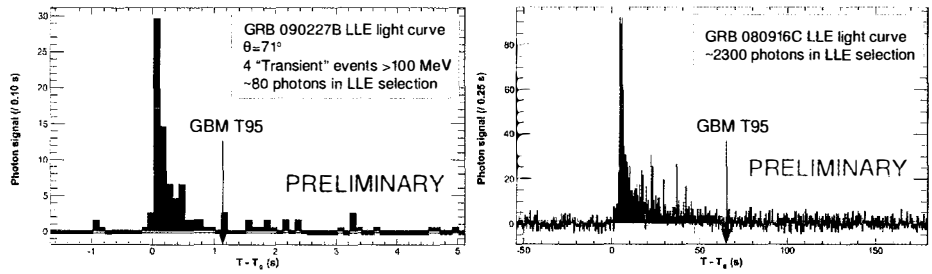

Figure 1: LAT Low-Energy (LLE) light curves of GRB 090227B (left) and GRB 080916C (right).

2.1 Ingredients for GRB Analysis with the LAT

Fermi was designed with the capability to repoint in the direction of a bright GRB and keep its position near the centre of the LAT FoV for several hours, subject to Earth-limb constraints. This repointing occurs autonomously in response to requests from the GBM or the LAT, with adjustable brightness thresholds. Each Autonomous Repoint Request (ARR) causes rapid variations of the source off-axis angle in the LAT FoV, making the estimate of the background quite challenging[a]. In particular, the usual background-estimation method which consists of extrapolating fits of the event rate before the burst (or interpolating from fits to pre- and post-burst time intervals) provides wrong estimates in the case of ARRs. For the analyses included in the LAT GRB catalog, we instead make use of the background-estimation tool developed by the LAT collaboration and described in detail in Ref. [1]. This tool works in any observational conditions and provides estimates with 10-15% accuracy.

Another important ingredient for GRB studies is the use of the "LAT Low-Energy" (LLE) event class[25]. In the catalog work, most GRBs are detected by performing an unbinned likelihood analysis based on the standard event selection (the so-called "transient"-class events) above 100 MeV. However, some GRBs are too weak or at too high off-axis angles (>70°) to be significantly detected. In order to recover significant signal in these situations, we introduced the LLE event class, which corresponds to relaxed event selection criteria. It provides significantly higher effective area at tens-of-MeV energies and at larger off-axis angles (Fig. 1, left) and, for the bright GRBs, the needed statistics to study the temporal properties at low energies in the LAT (Fig. 1, right).

2.2 Temporal and Spectral Properties

Whereas the GBM detects ~250 GRBs per year [24] (half of them occuring in the LAT FoV), the LAT detected 35 GRBs in 3 years of operations. This includes 30 long and 5 short GRBs, and 7 "LLE-only" GRBs. Approximately half of these detections benefited from more accurate follow-up localizations by Swift and ground-based observatories. In this sample, 10 redshift measurements are available, ranging from z=0.74 (GRB 090328) to z=4.35 (GRB 080916C).

The GRB emission detected by the LAT above 100 MeV is systematically delayed with respect to the emission observed with the GBM at hundreds-of-keV energies (Fig. 2, left), and it lasts systematically longer (Fig. 2, right). Joint spectral fits using GBM and LAT data recorded during the GBM T_{90} were possible for 30 LAT-detected GRBs and showed that the commonly used Band function [14] does not capture all spectral characteristics. While this phenomenological

[a]Another consequence is the huge variation of the LAT exposure, which strongly modulates the observed light curves in detected count space.

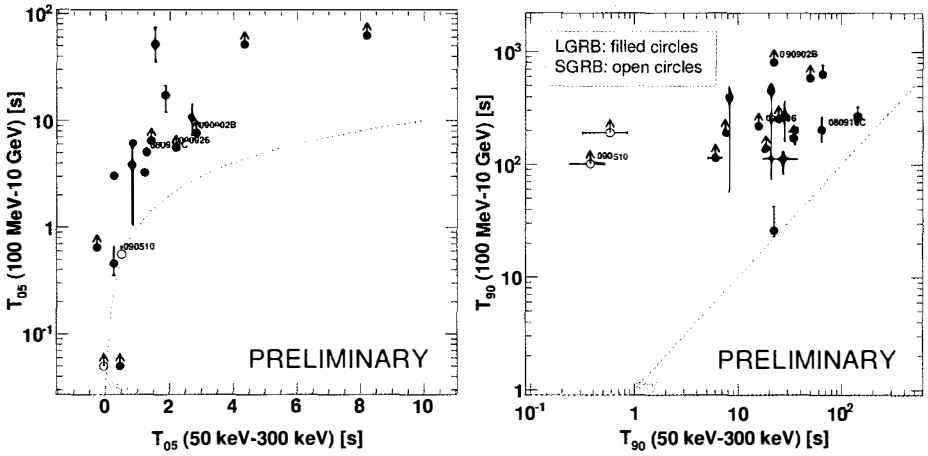

Figure 2: Onset time (T_{05}, left) and duration (T_{90}, right) of the GRB emission observed by the GBM (50-300 keV) and the LAT (>100 MeV). Filled circles indicate long GRBs, and open circles short GRBs.

shape alone can reproduce the spectrum of 21 GRBs in this sample, all other spectra but two (for which a logarithmic parabola alone is preferred) are best fitted using either an additional power-law component (6 GRBs[b]) and/or an exponential cutoff (2 GRBs) at high energies. Apart from the functional shapes examined in the LAT GRB catalog analysis, a couple of GRBs (e.g., GRB 110721A [13]) also show deviations from the Band function in the sub-100 MeV energy domain. This low-energy thermal component has been interpreted as the fireball photospheric emission and is thoroughly addressed in Ref. [23]. As for instance discussed in Ref. [26], understanding the GRB spectral diversity as revealed by *Fermi* will require detailed broad-band physical modeling in the future.

The origin of the high-energy emission seen in the LAT at later times is less unclear, as the LAT flux above 100 MeV decays smoothly after the end of the low-energy prompt emission (Fig. 3, left). In particular, no obvious pattern is seen in the spectral evolution, and the photon spectral index is close to -2. Such a decay phase is consistent with an afterglow origin of the high-energy emission. Specifically, the observed light curves are well described by a power law in all but three cases, for which a broken power law is preferred (Fig. 3, right). The significance of the breaks corresponds to a chance probability of less than 10^{-3}. In these cases (GRBs 090510, 090902B and 090926A), the time of the break is observed after the end of the low-energy emission, as measured by the GBM T_{90}. If we define a late time decay index α_L as the index measured after the break for these GRBs, and the index of the power law for the light curves which are best fitted by a simple power law, we find that $\alpha_L \simeq -1$. This value is expected from the standard afterglow model for an adiabatic expansion of the fireball in a constant density environment. Note that a radiative expansion would predict a decay index of $10/7$ [19], which is not observed. The initial steep decay phase observed in the light curves of GRBs 090510, 090902B and 090926A (Fig. 3, right) might be due to a transition from the prompt emission phase to the phase dominated by the early afterglow emission.

The afterglow of GRB 090510 and GRB 110731A was observed by Swift and other instruments when the high-energy emission was still detectable by the LAT. A broad-band study, from optical wavelengths to gamma rays, showed that the emission is compatible with being

[b]Including GRB 080916C, for which this detection was made possible thanks to the improvements in estimating the background and the instrument responses with respect to the initial analysis [2].

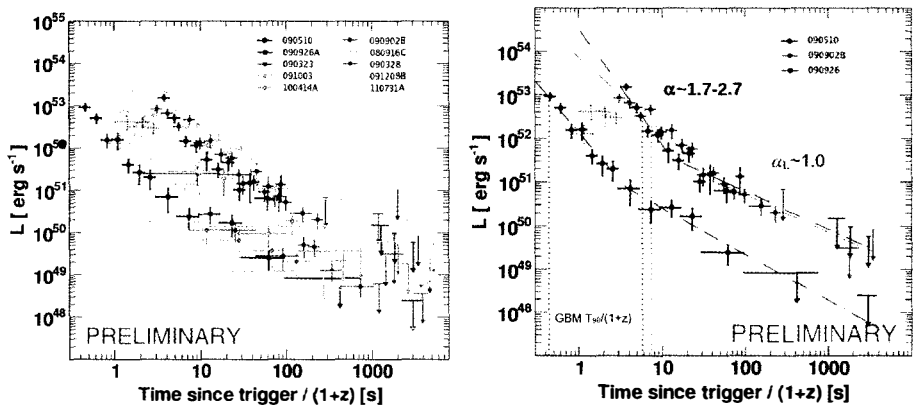

Figure 3. *(Left)* Decay of the luminosity with time measured in the rest frame for all the LAT GRBs with detected extended emission. *(Right)* Same quantity, for 3 GRBs with a significant time break detected. Dashed-dotted lines are the best fits of a broken power law to each light curve, while dashed crosses are the luminosities before the peak times (not used in the fits).

from external shock origin [17,10]. In one other case, GRB 100728A, high-energy emission was detected by the LAT in correspondence with and around an X-ray flare, which was successfully modeled from X-ray to gamma-ray energies as emission from internal shocks [6].

2.3 Fluences and Energetics

Fig. 4 (left) compares the fluence of the LAT GRBs in the GBM energy range and within the GBM T_{90} with the entire GBM spectral catalog sample [20]. Not surprisingly, the GRBs detected by the LAT are found to be among the GBM brightest GRBs[c]. In addition, remarkable properties of GRBs were discovered with the LAT at high energies. Firstly, whereas the fluence in the LAT energy range is ≈10% of the fluence in the GBM energy range for long GRBs, short GRBs have a larger fluence ratio (Fig. 4, right). Although this result certainly requires more GRB statistics to be firmly confirmed, it already suggests different energy outputs above 100 MeV from GRBs depending on their progenitors. Secondly, some evidence of a class of hyper-energetic GRBs was found, with four exceptionally bright events (GRBs 080916C, 090510, 090902B and 090926A)[2,7,3,8]. This important result can not be simply explained by the proximity of these GRBs, as their redshifts are distributed from 0.90 to 4.35.

Fig. 5 (left) compares the isotropic equivalent energy (from 1 keV to 10 MeV during the GBM T_{90}) of the 10 LAT GRBs with measured redshifts with the samples of GBM [20] and Swift [16] GRBs. It shows that the LAT GRBs are among the most (intrinsically and observationally) energetic GRBs (GRB 090510 being the most energetic short one), with no particular trend in redshift with respect to the GBM and Swift samples. The right panel in the same figure shows that the rest-frame emission from these GRBs can frequently reach several tens-of-GeV energies, which is a very good sign for the detection prospects of future very high-energy observatories such as the High Altitude Water Cherenkov experiment [27] and the Cherenkov Telescope Array [21]. These high-energy photons were extensively used to set different kinds of constraints. First of all, they provided lower limits on the mean Lorentz factor Γ of the GRB jets through compactness arguments (Fig. 6, right), and helped to demonstrate that both long and short GRBs can have high outflow rapidity [2,7,3,8], a key result for GRB modeling (see also section 3). Secondly,

[c]Note that selection effects due to ARRs should be investigated though.

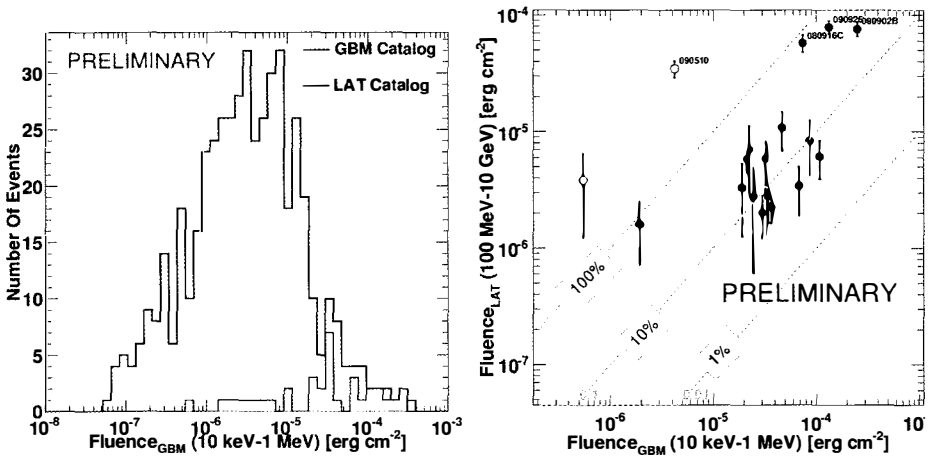

Figure 4: *(Left)* Fluence in the GBM energy range and within the GBM T_{90}, for the entire sample in the GBM spectral catalog and for the LAT GRBs only. *(Right)* Comparison of the LAT GRB fluences, computed in the GBM and LAT respective energy ranges and T_{90}'s. Filled circles indicate long GRBs, and open circles short GRBs.

high-energy gamma rays can be absorbed by the Extragalatic Background Light (EBL) when travelling from the emitting region to the observer. Only photons with energies above ~10 GeV suffer from pair creation on the EBL, and they can be used to probe this cosmic diffuse radiation field as a function of redshift in the optical-UV range[5]. Finally, the LAT observations of >10 GeV photons from bright GRBs also provided the best lower limits on the energy scale at which postulated quantum-gravity effects create violations of Lorentz invariance. These constraints strongly disfavour models which predict a linear variation of the speed of light with photon energy below the Planck energy scale (i.e., $<1.22\times10^{19}$ GeV)[4,28].

3 Non-Detections of GBM Bright GRBs and LAT GRB Rate

Whereas ~9.3 GRBs with more than 10 photons above 100 MeV were expected per year from pre-launch estimates[15], a mean LAT GRB rate of ~6.3 GRBs per year is obtained from the first LAT GRB catalog, based on the number of photons predicted by the likelihood analysis within the LAT T_{90} (Fig. 6, left). In spite of different systematic uncertainties arising in these analyses[d], the lack of LAT GRB detections raises the question whether the high-energy emission is suppressed and if spectral cutoffs are more common than anticipated, similarly to the attenuated spectrum of GRB 090926A[8].

In order to investigate this question, we estimated the fraction of GBM GRBs that should have been detected by the LAT. In the analysis presented in Ref.[9], we examined a sample of 30 GBM bright and hard GRBs, with >70 counts/s in the BGO detectors and with a good measurement of the high-energy slope β of the Band spectrum ($\Delta\beta$ <0.5). Comparing upper limits on the LAT flux (0.1-10 GeV) over the GBM T_{90} with predictions from the extrapolation of the spectral fits to GBM data, we found that ~50% (15 GRBs) should have been detected by the LAT. In a second step, we included the LAT data ("transient"-class events) above 100

[d]For instance, the extrapolations from the BATSE energy range to the LAT energy range as performed in Ref.[15] are uncertain due to the large lever arm and to errors on the high-energy spectral slope β. Moreover, these past estimates used simple detection thresholds and idealized backgrounds.

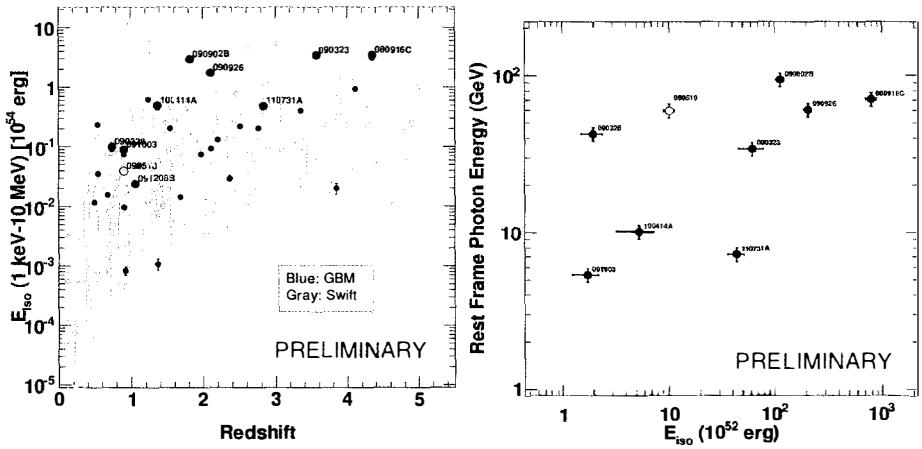

Figure 5: *(Left)* Isotropic equivalent energy from 1 keV to 10 MeV during the GBM T_{90}. The 10 LAT GRBs with measured redshifts are compared with the samples of GBM and Swift GRBs. *(Right)* Rest-frame energy of the highest-energy photons from the GRBs detected by the LAT.

MeV in the spectral fits, which yielded considerably softer β values and decreased this fraction down to ~23%. Finally, we repeated the GBM-LAT joint fits, adding a spectal softening in the model between the GBM/BGO and the LAT energy ranges. This modification to the spectrum improved the fits significantly for 20% of the GRBs (6 out of 30), implying that a degree of spectral softening is required to explain their LAT non-detection. The rest 80% of the GRBs remained statistically consistent with a softer β. It is interesting to note that these 6 GRBs have the smallest $\Delta\beta$ values (and no other particular characteristic), indicating that only a very accurate spectroscopy is sensitive to this spectral feature. Assuming that the softening is due to internal opacity effects, we finally set upper limits on the jet mean Lorentz factors of the 6 GRBs, assuming a (conservative) 100 ms variability time scale. The comparison of these limits to other estimates obtained for the 4 LAT brightest GRBs (Fig. 6, right) indicates a relatively broad range of possible Γ values among *Fermi* GRBs.

4 Conclusions and Perspective

The GBM and LAT instruments onboard the *Fermi* space observatory have jointly detected the keV-MeV-GeV emission from a large sample of GRBs. The first LAT GRB catalog [18] will certainly be a valuable tool for future theoretical research and a useful informational resource for scientists who wish to analyze LAT GRB data. The LAT detected 35 GRBs in the first 3 years of *Fermi* operations, by means of the standard likelihood technique above 100 MeV and/or using the new LAT Low-Energy (LLE) event class. A population study indicates (or confirms) interesting patterns, like the delayed onset and the temporal extension of GRB emission observed in the LAT above 100 MeV with respect to the emission detected by the GBM at lower energies. Emergent groups are also observed: LAT GRBs are among the brightest and most energetic GBM GRBs, and the evidence of a class of hyper-energetic GRBs is growing.

Before *Fermi*, the phenomenological Band function provided the standard picture of GRB spectra during their prompt emission phase. A so-called "Band model crisis" has been prompted by *Fermi*, which revealed the diversity and complexity in GRB spectra, calling for a better broad-band modeling, opening new questions and triggering new theoretical developments. The origin

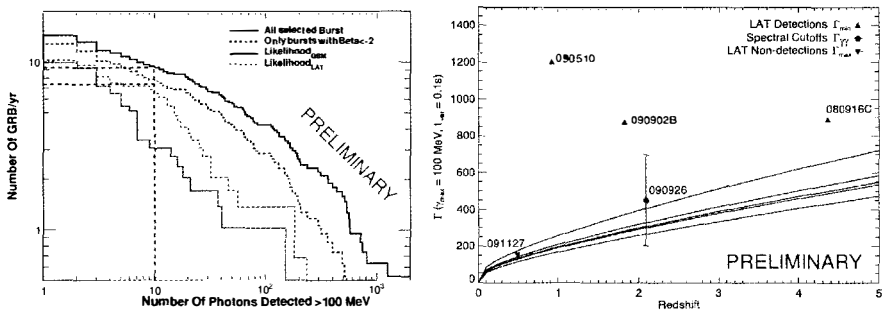

Figure 6: *(Left)* Comparison between the observed yearly rate of LAT GRB detections (red lines) to the pre-launch expectations (black lines) for an energy threshold of 100 MeV. The dashed black line corresponds to an input distribution from which hard bursts have been removed. The red lines indicate the observed number of GRBs as a function of the number of events predicted by the best-fit model in the likelihood analysis. The hatched regions correspond to the statistical uncertainties assuming Poisson fluctuations. *(Right)* Upper limits $\Gamma_{\rm max}$ on the jet mean Lorentz factors for the 6 GRBs exhibiting a spectral softening. We only know the redshift for GRB 091127 (brown triangle), so we set $\Gamma_{\rm max}(z)$ for the rest: GRBs 080925, 081207, 090131, 090528B, and 100724B (brown curves). Lower limits $\Gamma_{\rm min}$ (GRBs 080916C, 090510, 090902B) and measurements (GRB 090926A) for LAT bright GRBs are superimposed (blue triangles and point). The target photon field for $\gamma\gamma$ absorption is assumed uniform, isotropic and time-independent, but the error bar for GRB 090926A accounts for different models, illustrating the overall scaling that could be applied to the entire figure.

of the delayed onset of GRB emission observed in the LAT above 100 MeV remains unclear. At late times, the high-energy emission is consistent with the canonical afterglow model if considering an adiabatic fireball. Better time-resolved spectroscopic studies during the prompt emission phase and during the transition to the early afterglow phase will thus be crucial in order to discriminate between the existing models (leptonic vs. hadronic, internal vs. external shocks) which are commonly invoked to explain the GRB temporal and spectral properties at high energies.

Fewer GRBs are detected by the LAT than would be expected by extrapolating BATSE or GBM spectra. The need for an overall softer spectrum or for high-energy cutoffs in GRB spectra at MeV energies is confirmed (~20% in the sample examined). Assuming that this spectral softening arises from internal opacity effects, the range of values for the mean Lorentz factors Γ of *Fermi* GRB jets is found to be broader than those derived only from the LAT bright GRBs. More LAT GRBs will certainly help to understand these spectral properties and to shed light on the LAT GRB rate. The LLE data fill the gap between the GBM and the LAT energy ranges and have been publicly released at the *Fermi* Science Support Center [e]. Whereas the standard "transient" event selection runs out of effective area below ~100 MeV, the LLE event selection provides plenty of statistics to probe GRB spectral cutoffs in the tens-of-MeV-energy region. Major improvements of the standard analysis are also expected from the future "Pass 8" data, which correspond to a radical revision of the LAT event-level analysis based on the experience gained in the prime phase of the mission. In particular, these improvements include an increased effective area (2-3 times larger than "Pass 7" at 100 MeV) and an extension of the energy reach for the photon analysis below 100 MeV in the future [12].

Acknowledgments

The *Fermi* LAT Collaboration acknowledges generous ongoing support from a number of agencies and institutes that have supported both the development and the operation of the LAT as

[e] http://heasarc.gsfc.nasa.gov/W3Browse/fermi/fermille.html

well as scientific data analysis. These include the National Aeronautics and Space Administration and the Department of Energy in the United States, the Commissariat l'Energie Atomique and the Centre National de la Recherche Scientifique / Institut National de Physique Nuclaire et de Physique des Particules in France, the Agenzia Spaziale Italiana and the Istituto Nazionale di Fisica Nucleare in Italy, the Ministry of Education, Culture, Sports, Science and Technology (MEXT), High Energy Accelerator Research Organization (KEK) and Japan Aerospace Exploration Agency (JAXA) in Japan, and the K. A. Wallenberg Foundation, the Swedish Research Council and the Swedish National Space Board in Sweden.

Additional support for science analysis during the operations phase is gratefully acknowledged from the Istituto Nazionale di Astrofisica in Italy and the Centre National d'Etudes Spatiales in France.

References

1. A.A. Abdo *et al*, ApJ **707**, 580 (2009).
2. A.A. Abdo *et al*, Science **323**, 1688 (2009).
3. A.A. Abdo *et al*, ApJ Letters **706**, 138 (2009).
4. A.A. Abdo *et al*, Nature **462**, 331 (2009).
5. A.A. Abdo *et al*, ApJ **723**, 1082 (2010).
6. A.A. Abdo *et al*, ApJ Letters **734**, 27 (2011).
7. M. Ackermann *et al*, ApJ **716**, 1178 (2010).
8. M. Ackermann *et al*, ApJ **729**, 114 (2010).
9. M. Ackermann *et al*, ApJ **754**, 121 (2012).
10. M. Ackermann *et al*, ApJ **763**, 71 (2013).
11. W.B. Atwood *et al*, ApJ **697**, 1071 (2009).
12. W.B. Atwood *et al*, *2012 Fermi Symposium, eConf Proceedings C121028* (arXiv:1303.3514).
13. M. Axelsson *et al*, ApJ Letters **757**, 31 (2011).
14. D.L. Band *et al*, ApJ **413**, 281 (1993).
15. D.L. Band *et al*, ApJ **701**, 1673 (2009).
16. N.R. Butler *et al*, ApJ **671**, 656 (2007).
17. M. De Pasquale *et al*, ApJ Letters **709**, 146 (2010).
18. *Fermi* LAT Collaboration, *submitted to ApJS* (arXiv:1303.2908).
19. G. Ghisellini *et al*, MNRAS **403**, 926 (2010).
20. A. Goldstein *et al*, ApJS **199**, 19 (2012).
21. G. Lamanna, *this conference.*
22. C. Meegan *et al*, ApJ **702**, 791 (2009).
23. E. Moretti, *this conference.*
24. W.S. Paciesas *et al*, ApJS **199**, 18 (2012).
25. V. Pelassa *et al*, *2009 Fermi Symposium, eConf Proceedings C091122* (arXiv:1002.2617).
26. R. Preece, *this conference.*
27. K. Tollefson, *this conference.*
28. V. Vasileiou *et al*, *accepted for publication in Phys. Rev.* D (arXiv:1305.3463).